NUMERICAL SIMULATION OF WATERJET EXCAVATION IN ROCK USING SPH METHOD

Masayuki SHOJI

1. INTRODUCTION

Recently, an increase of greenhouse gas and the exhaustion of fossil fuels are important issues. Therefore, renewable energy and alternative energy taken from deep underground have been paid great attention to. Waterjet is suitable for an excavation technology to extract energy that exists deep underground. However, since the performance of waterjet technologies depends on many parameters, many experiments are required to develop a waterjet technology. Thus, numerical simulation of waterjet excavation in rock can help decreasing the development cost. Because both solid and liquid are greatly deformed in waterjet excavation, it is difficult to model this problem by using a finite element method.

The smoothed particle hydrodynamics (SPH) is a fully Lagrangian technique in which the numerical solution is achieved without grid. An advantage of the SPH is the relative ease with which new physics may be incorporated into the formulation. It is also straightforward to allow boundaries to move or deform and to model the interaction between fluid and solid, and to extend to three dimensions. There have been some studies on the SPH simulation for waterjet cutting, but there is no research on rock.

In this study, I aimed to develop a simulation method for waterjet excavation in rock using the SPH method based on real excavation mechanism for rock. The contents of this study are as follows:

1) Experiment of waterjet excavation in rock.
2) Modeling of waterjet and rock for the SPH method.
3) Comparison of the simulation result on waterjetting to a rigid block with the experimental result of waterjetting to a steel plate.
4) Comparison of the simulation results on waterjet rock excavation based on five failure criterions with the experimental results.
5) Simulation on the effect of Young's modulus of rock.

2. MODELING BY SPH

2.1 Basic ideas of SPH

For a given function $\phi(\boldsymbol{r})$, the expression of particle approximation by using kernel function $\langle\langle \phi(\boldsymbol{r}) \rangle\rangle$ is defined as

$$\langle \phi(\boldsymbol{r}) \rangle = \int_{\Omega} \phi(\boldsymbol{r}') W(\boldsymbol{r} - \boldsymbol{r}', h) d\boldsymbol{r}', \tag{1}$$

where Ω is the volume of the object; $\boldsymbol{r}$ is the current position vectors; h is called smoothing length that controls the influence domain, and $W(\boldsymbol{r} - \boldsymbol{r}', h)$ is kernel function (Fig. 1), which must satisfy the following three properties:

$$\lim_{h \to 0} W(\boldsymbol{r} - \boldsymbol{r}', h) = \delta(\boldsymbol{r} - \boldsymbol{r}'), \tag{2}$$

$$\int_{\Omega} W(\boldsymbol{r} - \boldsymbol{r}', h) d\boldsymbol{r}' = 1, \tag{3}$$

$$W(\boldsymbol{r} - \boldsymbol{r}', h) = 0 \quad \text{for} \quad |\boldsymbol{r} - \boldsymbol{r}'| \geq h. \tag{4}$$

In this study, the cubic spline interpolation function was used as kernel function.

In the SPH method, the calculation domain is represented by N points (particles), which carry mass and field variable information such as density, stress, etc. Accordingly, the continuous integral representation for $\phi(\boldsymbol{r})$ is approximated, and the particle approximation ϕ_i at particle i can be written as

$$\phi_i = \sum_{j}^{N} m_j \frac{\phi_j}{\rho_j} W_{ij}, \tag{5}$$

where m_j is the mass and ρ_j is the density of the jth particle, and $W_{ij} = W(\boldsymbol{r}_i - \boldsymbol{r}_j, h)$.

Following the same argument, the particle approximation for the spatial derivative of the function at particle i is

$$\left(\frac{\partial \phi}{\partial x^{\alpha}} \right)_i = \sum_{j}^{N} m_j \frac{\phi_j}{\rho_j} \frac{\partial W_{ij}}{\partial x^{\alpha}}, \tag{6}$$

where x^{α} is the orthogonal coordinate axis, and the Greek superscripts denote the spatial coordinate directions.

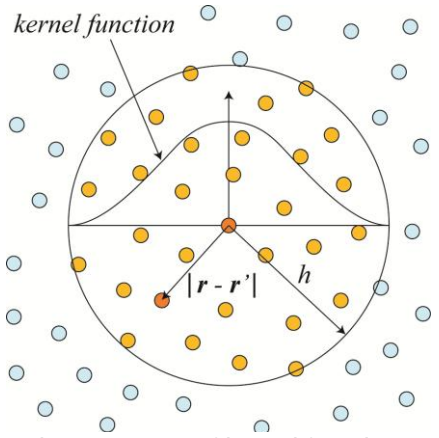

Fig.1 Concept of kernel function.

2.2 Modeling of waterjet

Waterjet is assumed to be a viscous fluid with weak compressibility. The governing equations are the equations of continuity, motion and state, as given by

$$\frac{D\rho}{Dt} = -\rho \frac{\partial v^{\alpha}}{\partial x^{\alpha}}, \tag{7}$$

$$\frac{Dv^{\alpha}}{Dt} = \frac{1}{\rho}\frac{\partial \sigma^{\alpha\beta}}{\partial x^{\beta}} + f^{\alpha}, \tag{8}$$

$$P = B\left[\left(\frac{\rho}{\rho_0}\right)^{\gamma} - 1\right], \tag{9}$$

where t is time, v^{α} is the velocity vector, $\sigma^{\alpha\beta}$ is the total stress tensor, f^{α} is the external force, P is pressure, ρ_0 is initial density, $\gamma = 7$ and B is a constant related to the bulk modulus of elasticity of the fluid.

The stress tensor consists of two parts: pressure term and viscous term,

$$\sigma^{\alpha\beta} = -P\delta^{\alpha\beta} + \mu T^{\alpha\beta}, \tag{10}$$

where μ is the dynamic viscosity and $T^{\alpha\beta}$ is the shear strain rate.

Converting and applying the SPH particle approximation to the Eqs. (7) and (8), the equations of continuity and motion on particle i in the SPH formulation are

$$\frac{D\rho_i}{Dt} = \sum_j^N m_j \left(v_i^{\alpha} - v_j^{\alpha}\right)\frac{\partial W_{ij}}{\partial x^{\alpha}}, \tag{11}$$

$$\frac{Dv^{\alpha}}{Dt} = \sum_j^N m_j \left(\frac{\sigma_i^{\alpha\beta}}{\rho_i^2} + \frac{\sigma_j^{\alpha\beta}}{\rho_j^2}\right)\frac{\partial W_{ij}}{\partial x^{\beta}} + f_i^{\alpha}. \tag{12}$$

2.3 Modeling of rock materials

Modeling the behavior of rock using the SPH method is similar to that of water. Since rock is assumed to be elastic, Hooke's law is used for the equation of state,

$$P = K\eta = K\left(\frac{\rho}{\rho_0} - 1\right), \tag{13}$$

where K is bulk modulus, and η is the volumetric strain.

Eqs. (12) and (13) are also used to estimate the density and motion of rock particles. However, the stress tensor does not include the viscosity term, but includes the deviatoric stress,

$$\sigma^{\alpha\beta} = -P\delta^{\alpha\beta} + s^{\alpha\beta}. \tag{14}$$

The deviatoric stress $s^{\alpha\beta}$ can be estimated using the Jaumann stress rate,

$$\dot{s}^{\alpha\beta} = 2G\left(\dot{\varepsilon}^{\alpha\beta} - \frac{1}{3}\delta^{\alpha\beta}\dot{\varepsilon}^{\gamma\gamma}\right) + s^{\alpha\gamma}\omega^{\beta\gamma} + s^{\gamma\beta}\omega^{\alpha\gamma}, \tag{15}$$

where G is the shear modulus, $\dot{s}^{\alpha\beta}$ is the deviatoric stress rate, $\dot{\varepsilon}^{\alpha\beta}$ is the strain rate tensor and $\omega^{\alpha\beta}$ is the rotation tensor.

2.4 Artificial viscosity

To prevent unphysical penetration of particles, an artificial viscosity has been introduced to the pressure term in the equation of motion. Artificial viscosity Π_{ij} is defined as

$$\Pi_{ij} = \begin{cases} \dfrac{-\alpha \bar{c}_{ij}\lambda_{ij} + \beta\lambda_{ij}^2}{\bar{\rho}_{ij}} & \boldsymbol{v}_{ij}\cdot\boldsymbol{r}_{ij} < 0 \\ 0 & \boldsymbol{v}_{ij}\cdot\boldsymbol{r}_{ij} \geq 0 \end{cases}, \tag{16}$$

where

$$\lambda_{ij} = \frac{\bar{h}_{ij}\boldsymbol{v}_{ij}\cdot\boldsymbol{r}_{ij}}{\boldsymbol{r}_{ij}^2 + \varphi^2}, \tag{17}$$

$$\boldsymbol{v}_{ij} = \boldsymbol{v}_i - \boldsymbol{v}_j, \quad \boldsymbol{r}_{ij} = \boldsymbol{r}_i - \boldsymbol{r}_j. \tag{18}$$

In the above equations, v and c represent the particle velocity vector and the speed of sound. The factor $\phi = 0.1h$ is inserted to prevent numerical divergences when two particles are approaching each other. Bars denote the mean value, and α and β are constants. In this study, there values were set to $\alpha = 0.01$ and $\beta = 0$ for water and $\alpha = 2.5$ and $\beta = 2.5$ for rock.

3. ROCK EXCAVATION AND FAILURE CRITERION

3.1 Excavation experiment

To verify the simulation results, an experiment of waterjet excavation was conducted. Kimachi sandstone was used as a specimen. The nozzle diameter was 1 mm, the driving pressure was 30 MPa (velocity = 25 m/s) and the standoff distance was 5.0 mm.

Fig. 2 shows a cross-sectional view of a borehole obtained by 5 sec jetting. It is observed that the borehole mouth is enlarged. This indicates that the returning jet flow erodes the wall of the borehole mouth.

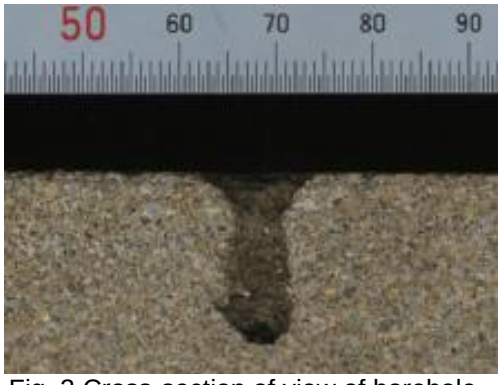

Fig. 2 Cross-section of view of borehole.

3.2 Failure criterion

In this study, it was assumed that a rock particle fails when the particle satisfy a fracture criterion, and the failed particle is subjected only to pressure. As the failure criterion, the following five criterions were used:

1) Particle fails when the tensile strain exceeds a critical value (tensile strain criterion).
2) Particle fails when the travel distance exceeds a critical value (travel distance criterion).
3) Particle fails when the equivalent strain exceeds a critical value (equivalent strain criterion).
4) Particle fails when the stress exceeds a critical value (stress criterion).
5) Particle fails when the Mohr-Coulomb failure criterion is satisfied (the Mohr-Coulomb criterion).

4. RESULTS AND DISCUSSION

Table 1 shows the conditions of simulation.

4.1 Jetting to a rigid body

To verify modeling of waterjet, an experiment on waterjetting to a steel plate was conducted on the condition that the driving pressure is 30 MPa and the standoff distance is 5.0 mm. Fig. 3 shows the experimental result of jetting to a steel plate. Fig. 4 shows the result of simulation on waterjetting to a rigid body. Water was splashed similarly in both results. Consequently, modeling of waterjet has proved to be correct.

4.2 Influence of the failure criterion

Figs. 5 and 6 show the results for the tensile strain criterion and for the travel distance criterion, respectively. It is observed that the mouth of boreholes was enlarged, similar to the experimental result. Fig 7 shows the result for the equivalent strain criterion. Macroscopic fractures are observed. Figs. 8 and 9 show the results for the stress criterion and the Mohr-Coulomb failure criterion, respectively. It is observed that many failed particles were compressed to rock particles. Excavation was successfully simulated for all criterions.

4.3 Influence of Young's modulus

Figs. 10 and 11 show the results when Young modulus is 1.0 GPa and 10 GPa, respectively. Both boreholes have a similar depth. This is because it is easier to exhaust the failed particles for the harder rock.

Table 1 Analysis conditions.

Density of water, ρ_w [kg/m^3]	1000
Viscosity of water μ [Ns/m^2]	0.001
Density of rock, ρ_r [kg/m^3]	2500
Poisson ratio of rock, ν [–]	0.3
Flow speed of water jet V_{jet} [m/s]	200
Water jet nozzle diameter d_n [mm]	1.0
Standoff distance, x [mm]	5.0

Fig. 3 Experimental result of jetting to a steel plate.

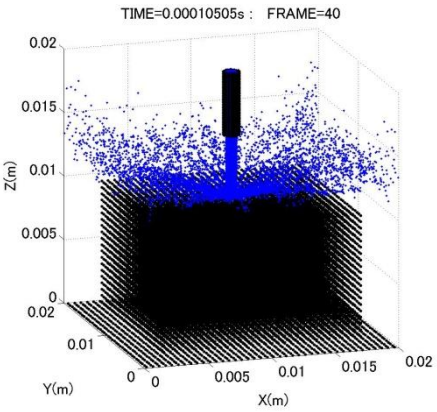

Fig. 4 Analysis result of jetting to a rigid body.

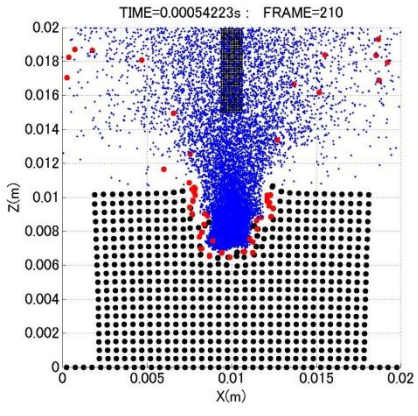

Fig. 5 Result for the tensile strain criterion.

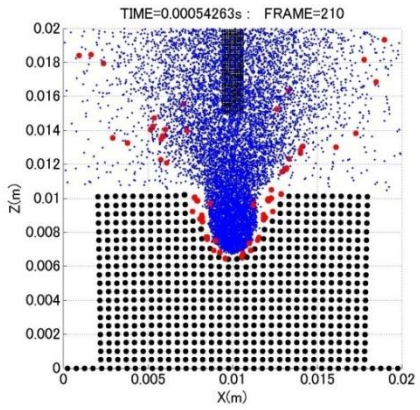

Fig. 6 Result for the traveling distance criterion.

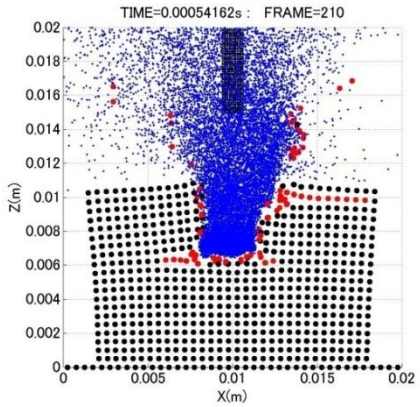

Fig. 7 Result for the equivalent strain criterion.

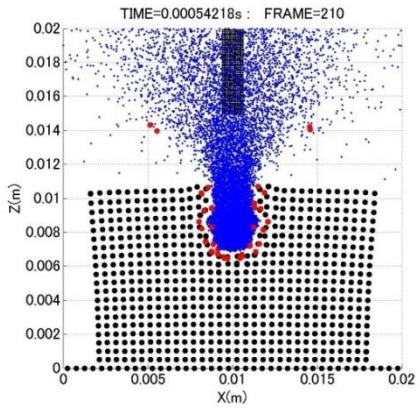

Fig. 8 Result for the stress criterion.

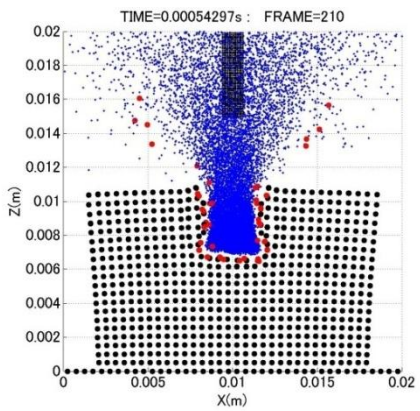

Fig. 9 Result for the Mohr-Coulomb criterion.

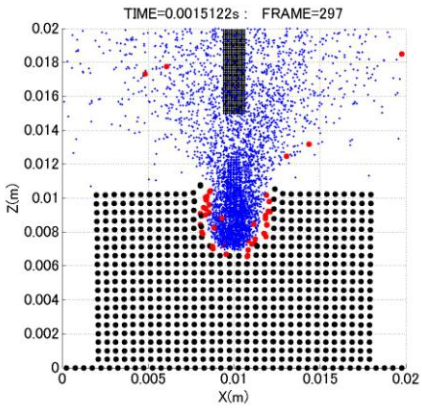

Fig. 10 Result for Young's modulus of 1.0 GPa.

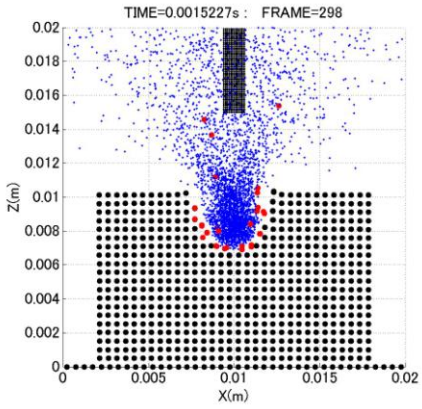

Fig. 11 Result for Young's modulus of 10 GPa.

5. CONCLUSIONS

Main results obtained in this study can be summarized as follows:

1) The SPH simulation result of waterjetting to a rigid body showed the behavior of waterjet similar to the experimental result.
2) Waterjettting to rock was simulated based on five failure criterions and all results reproduced excavation successfully.
3) The tensile strain criterion and the travel distance criterion showed results similar to the experimental result.
4) The borehole in rock with Young's modulus of 10 GPa was as deep as that of 1.0 GPa, since it is easier to exhaust the broken particles for the harder rock.

REFERENCES

[1] J. J. Monaghan, An introduction to SPH, Computer Physics Communications 48 (1988) 89-96

[2] M. G. Gesteira *et al*, SPHysics